BACHELOR'S DEGREE THESIS

Degree in Mathematics

Title: Dynamics and bifurcations in a simple quasispecies model of unstable tumorigenesis

Author: Vanessa Castillo Blanco

Advisors: Josep Sardanyés Cayuela[†]
José Tomás Lázaro Ochoa[*]

Department: Complex Systems Lab (PRBB, UPF)[†]
Institut de Biologia Evolutiva (CSIC-UPF)[†]
Departament de Matemàtica Aplicada I[*]

Academic year: 2014

UNIVERSITAT POLITÈCNICA DE CATALUNYA
BARCELONATECH
Facultat de Matemàtiques i Estadística

Abstract

Cancer is a complex disease and thus is complicated to model. However, simple models that describe the main processes involved in tumoral dynamics, e.g., competition and mutation, can give us clues about cancer behaviour, at least qualitatively, also allowing us to make predictions. Here we analyse a simplified quasispecies mathematical model given by ODEs describing the behaviour of tumor cells populations. We find the equilibrium points, also characterizing their stability and bifurcations focusing on the study of replication and mutation parameters. We identify a transcritical bifurcation at increasing mutation rates of the tumor cells population. Such a bifurcation involves an scenario with dominance of healthy cells and impairment of tumor populations. Finally, we characterize the transient time for this scenario, showing that a slight increase beyond the critical mutation rate may be enough to have a fast response during mutagenic therapies.

Contents

List of Figures

1 Introduction

Cancer is commonly viewed as a microevolutionary process [1, 2]. Genomic instability seems to be a common trait in most types of cancer [3] and is a key ingredient in the Darwinian exploratory process required to overcome selection barriers. By displaying either high levels of mutation or chromosomal aberrations, cancer cells can generate a progeny of highly diverse phenotypes able to evade such barriers [4]. Genomic instability refers to an increased tendency of alterations in the genome during the life cycle of cells. Normal cells display a very low rate of mutation (1.4×10^{-10} changes per nucleotide and replication cycle). Hence, it has been proposed that the spontaneous mutation rate in normal cells is not sufficient to account for the large number of mutations found in human cancers. Indeed, studies of mutation frequencies in microbial populations, in both experimentally induced stress and clinical cases, reveal that mutations that inactivate mismatch repair genes result in $10^2 - 10^3$ times the background mutation rate [5, 6, 7]. Also, unstable tumours exhibiting the so-called mutator phenotype [4] have rates that are at least two orders of magnitude higher than in normal cells [8, 9]. This difference leads to cumulative mutations and increased levels of genetic change associated to further failures in genome maintenance mechanisms [10]. The amount of instability is, however, limited by too high levels of instability, which have been suggested to exist in tumor progression [3], thus indicating that thresholds for instability must exist. In fact, many anti-cancer therapies take indirectly advantage of increased genomic instability, as is the case of mitotic spindle alteration by taxol or DNA damage by radiation or by alkilating agents.

The mutator phenotype is the result of mutations in genes which are responsible of preserving genomic stability, e.g., BRCA1 (breast cancer 1), BLM (bloom syndrome protein), ATM (ataxia telangiectasia mutated) or gene protein P53 (which is involved in multitude of cellular pathways such as cell cycle control, repair of DNA, among others). This mutator phenotype undergoes increases in mutation rates and can accelerate genetic evolution in cancer cells that can ultimately drive to tumor progression [4]. As mentioned,

genomic instability is a major driving force in tumorigenesis. Tumorigenesis can be viewed as a process of cellular evolution in which individual preneoplastic or tumor cells acquire mutations that can increase proliferative capacity and thus confer a selective advantage in terms of growth speed. The rate of replication of tumor cells can increase due to mutations in both tumor suppressor genes, e.g., APC (adenomatous polyposis coli) or P53 and oncogenes, e.g., RAS (rat sarcoma) or SRC. Tumor suppressor genes protect cells from one step on the path to cancer and oncogenes are genes that, when mutated, have the potential to cause cancer. In terms of population dynamics, alterations in both types of genes drive to neoplastic process through increases in cancer cells numbers. Mutations in replication-related genes that confer an increase of fitness and thus a selective advantage are named driver mutations [11]. This evolutionary process allows tumor cells to escape the restrictions that limit growth of normal cells, such as the constraints imposed by the immune system, adverse metabolic conditions or cell cycle checkpoints.

The iterative process of mutation and selection underlying tumor growth and evolution promotes the generation of a diverse pool of tumor cells carrying different mutations and chromosomal abnormalities. In this sense, it has been suggested that the high mutational capacity of tumor cells, together with an increase of proliferation rates, may generate a highly diverse population of tumor cells similar to a quasispecies [12, 13]. A quasispecies is a "cloud" of genetically related genomes around the so-called master sequence, which is at the mutation-selection equilibrium [14, 15]. Due to the heterogeneous population structure, selection does not act on a single mutant but on the quasispecies as a whole. The most prominent examples of a quasispecies are given by RNA viruses (e.g. Hepatitis C virus [16], vesicular stomatitis virus, the human immunodeficiency virus [17]...).

An important concept in quasispecies theory is the so-called error threshold [14, 15]. The error threshold is a phenomenon that involves the lost of information at high mutation rates. According to Eigen's original formulation, a quasispecies can remain at equilibrium despite at high mutation rates, but the surpass of the critical mutation rate will upset this balance since the master sequence itself disappears and its genetic information is lost due to the accumulation of errors. It has been suggested that many RNA viruses replicate

near the error threshold. [18]. Another important concept in quasispecies theory is lethal mutagenesis. As a difference from the error threshold (which is a shift in sequence space), lethal mutagenesis is a process of demographic extinction due to an unbearable number of mutations [19, 20]. Most basically, it requires that deleterious mutations are happening often enough that the population cannot maintain itself, but it is otherwise no different from any other extinction process in which fitness is not great enough for one generation of individuals to fully replace themselves in the next generation. In simple words, increased mutagenesis could impair the maintainance of a quasispecies due to the crossing of the error threshold or to lethal mutagenesis.

Quasispecies theory has provided a population-based framework for understanding RNA viral evolution [21]. These viruses replicate at extremely high mutation rates and exhibit significant genetic diversity. This diversity allows a viral population to rapidly adapt to dynamic environments and evolve resistance to vaccines and antiviral drugs. As we previously mentioned, several features have been suggested to be shared between RNA viruses and tumors [22], at least qualitatively. One is the presence of high levels of heterogeneity, both at genotype and phenotype levels. Typically, cancer cells suffer mutations affecting cell communication, growth and apoptosis (i.e., programmed cell death). Accordingly, escape from the immune system (and other selection barriers) operates in both RNA viruses and tumors. Viruses use antigenic diversity whereas tumors evade the immune system by loosing their antigens through mutation, or making use of antigenic modulation and/or tumor-induced immune suppression. Even more, similarly to RNA viruses, genetic instability in cancer cells will have detrimental effects on cells fitness, since most random mutations are likely to be harmful. As indicated by Cahill et al. [3], the best chance of cure advanced cancers might be a result of tumor genetic instability: cancer cells are more sensitive to stress-inducing agents. In this sense, possible therapies increasing mutation of tumor cells could push this populations towards the error threshold or induce lethal mutagenesis. This is the topic that we will address in this work by using a mathematical model describing the dynamics of competition between different cell populations with different levels of genomic instability.

2 Motivation and goals

The scope of this work is to describe the behaviour of a population of tumor cells with a simple mathematical model. It is worth saying that parameters play an important role in this model since they can give us different scenarios where tumor populations are suppressed or have low densities. Furthermore, changes between these different scenarios can be studied through the bifurcations of the system. So, the mathematical goals of the present study are:

- *Find equilibrium points.* We find their analytical expression and then we integrate the equations with an iterative method until the system reaches one of them.
- *Characterize the stability of the fixed points.* In order to do it, we need to compute the eigenvalues of a three dimension square matrix. We can find them both analytically and numerically.
- *Study the bifurcations.* We are concerned with possible changes in the stability of the fixed points as a function of the mutation rate and the fitness of cells populations.
- *Numerical computation of the transient times of the system.* We seek for an approximated law which give an idea of the velocity employed by the system to reach a given equilibrium state.

Each of the mathematical results will be given in terms of the mutation rates or the replication fidelity of the cells. This is important to understand how tumor populations behave. As we mention in the introduction, unstable cells can reach an error threshold and start loosing genetic information until its population decreases or, even more, disappears. We will see how mutation rates affect this error threshold. Furthermore, we will see how they affect to the velocity of the tumor population to reach an equilibrium point, which is interesting since mutation rates can be modified through drugs (similarly to RNA viruses [23]) or radiotherapy.

3 The model

In this section we introduce the model by Solé and Deisboeck [24] , which describes the competitive behaviour between cell populations with different levels of genomic instability. The model is given by the following set of differential equations:

$$\begin{cases} \dot{x_0} &= f_0 Q x_0 - \Phi(x_0, x_1, x_2) x_0, \\ \dot{x_1} &= f_0(1-Q)x_0 + f_1 Q' x_1 - \Phi(x_0, x_1, x_2) x_1, \\ \dot{x_2^i} &= f_1(1-Q')q_i' x_1 + \sum_{j=1}^{n} f_2^i \mu_{ij} x_2^i - \Phi(x_0, x_1, x_2) x_2^i. \end{cases}$$

Variable x_0 is the fraction of cells with anomalous growth but no genetic instability; x_1 is the fraction of cells derived from x_0 by mutation that allows genetic instability; and x_2^i for $i = 1, 2..., n$, is the fraction of tumor mutant cells that can be generated from x_1 due to mutation (see Fig. 1). Thus, x_0, x_1 and x_2^i denote the ratio of each population and, therefore, the sum of all these variables must be exactly one, i.e., $x_0 + x_1 + \sum_{i=1}^{n} x_2^i = 1$.

Moreover, the probability of mutation from x_1 to x_2^i can be denoted by $\mu_{x_1 \to x_2^i}$ and is given by $(1-Q')q_i'$. Notice that $\sum_{i=1}^{n} q_i' = 1$. Coefficients μ_{ij} denote the mutation rate (or probability) from x_2^j to x_2^i. The probability of error-free replication of x_2^i is represented by μ_{ii}.

Additionally, cross-mutations connect the different subclones of x_2 through the term $\sum_{j=1}^{n} f_2^j \mu_{ij} x_2^j$, where μ_{ij} indicate the mutation rate from x_2^j to x_2^i, f_j is the growth rate of each population and f_2^i the growth rate of each subpopulation of x_2. These f_j and f_2^i are known as the fitness of each population. The greater is the fitness of a population, the greater is its growth.

Finally, the term $\Phi(\mathbf{x})$ is the average fitness of the population vector $\mathbf{x} = (x_0, x_1, x_2^1, x_2^2, ..., x_2^n)$, i.e., $\Phi(\mathbf{x}) = f_0 x_0 + f_1 x_1 + \sum_{i=1}^{n} f_2^i x_2^i$. $\Phi(\mathbf{x})$ is also known as the "constant population constraint" and it ensures that the population remains constant, also introducing competition between the three populations of cells.

Although the model does not explicitly consider environmental constraints, such as

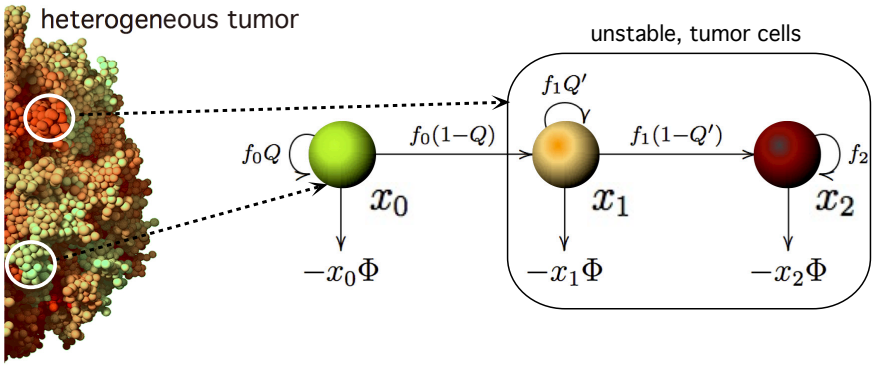

Figure 1: Schematic diagram of the investigated system. We consider a simple model of tumor growth describing the dynamics of competition between different cell populations with different levels of genomic instability. Three different cell populations are considered: x_0 represents anomalous growth but low genomic instability, and both x_1 and x_2 have larger genomic instabilities (see section 3 for a description of the model parameters).

blood supply, hypoxia or acidosis, they can be considered as implicitly introduced through the set $\{f_j\}_{j=0,1,2}$ [12].

The effect of mutations can be represented by means of a directed graph as shown in Fig. 1. Namely, x_0 mutates to x_1 with a probability of $\mu_0 = 1 - Q$. In the same way, x_1 mutates in different x_2^i-sequences with a probability $\mu_1 = 1 - Q'$. In both cases, $0 < Q, Q' < 1$, being Q and Q' the copying fidelity during replication for x_0 and x_1 respectively. So, in this model, mutations from x_1 to x_0 and from x_2^i to x_1 have not been considered. It is also worth noticing that the model with $Q' = 1$ is the two-variable quasispecies model [25].

The set of equations (1) can also be written in a matricial way:

$$\begin{pmatrix} \dot{x_0} \\ \dot{x_1} \\ \dot{x_2^1} \\ \vdots \\ \dot{x_2^n} \end{pmatrix} = \begin{pmatrix} f_0Q & 0 & 0 & \cdots & 0 \\ f_0(1-Q) & f_1Q' & 0 & \cdots & 0 \\ 0 & f_1(1-Q')q_1' & & & \\ \vdots & \vdots & & M_\mu D_{f_2} & \\ 0 & f_1(1-Q') & & & \end{pmatrix} \begin{pmatrix} x_0 \\ x_1 \\ x_2^1 \\ \vdots \\ x_2^n \end{pmatrix} - \Phi(\mathbf{x}) \begin{pmatrix} x_0 \\ x_1 \\ x_2^1 \\ \vdots \\ x_2^n \end{pmatrix} \qquad (1)$$

where $M_\mu = \begin{pmatrix} \mu_{11} & \cdots & \mu_{1n} \\ \vdots & & \vdots \\ \mu_{n1} & \cdots & \mu_{nn} \end{pmatrix}$ and $D_{f_2} = \begin{pmatrix} f_2^1 & & \\ & \ddots & \\ & & f_2^n \end{pmatrix}$

So, if we set M and D_f as the following matrices

$$M = \begin{pmatrix} Q & 0 & 0 & \cdots & 0 \\ 1-Q & Q' & 0 & \cdots & 0 \\ 0 & (1-Q')q_1' & & & \\ \vdots & \vdots & & M_\mu & \\ 0 & (1-Q') & & & \end{pmatrix}, D_f = \begin{pmatrix} f_0 & & & & \\ & f_1 & & & \\ & & f_2^1 & & \\ & & & \ddots & \\ & & & & f_2^n \end{pmatrix}$$

then M is a Markov matrix by columns. This means that $\sum_{i=1}^{n+2} M_{ij} = 1 \; \forall j = 1 \div n+2$. This kind of matrix appears in mathematical models in biology [28], economics (e.g., the Markov Switching Multifractal asset pricing model [29]), telephone networks (the Viterbi algorithm for error corrections [30]) or "rankings" as the PageRank algorithm from Google [31, 32]. Therefore, the system can be rewritten as:

$$\dot{\mathbf{x}} = MD_f\mathbf{x} - \Phi(\mathbf{x})\mathbf{x} \tag{2}$$

Our approach to this problem consists on assuming $\{x_2^i\}$ behaves as an average variable $x_2 = \sum_{i=1}^{n} x_2^i$. As a consequence, only two different mutation rates are involved in such simplified system: $\mu_0 = 1 - Q$ and $\mu_1 = 1 - Q'$. Then the set of equations remains to be:

$$\begin{cases} \dot{x_0} = f_0 Q x_0 - \Phi(x_0, x_1, x_2)x_0 \\ \dot{x_1} = f_0(1-Q)x_0 + f_1 Q' x_1 - \Phi(x_0, x_1, x_2)x_1 \\ \dot{x_2} = f_1(1-Q')x_1 + f_2 x_2 - \Phi(x_0, x_1, x_2)x_2 \end{cases} \tag{3}$$

From now on, let us assume that we always start with a population entirely composed by stable cells, i.e., $x_0 = 1$ and $x_1 = x_2 = 0$. Notice that for this particular case every point of the trajectory always verifies $x_0 + x_1 + x_2 = 1$.

4 Results and discussion

4.1 Equilibrium points

The system (3) has three different fixed points. Namely, a first one showing the total dominance of the unstable population, i.e., x_0 and x_1 go extinct and then $x_2 = 1$. A second one where x_0 goes extinct and x_1 coexists with x_2, and the third possible fixed point, where the three populations coexist. We can not consider a fixed point with $x_0 \neq 0$, $x_2 \neq 0$ and $x_1 = 0$ neither because, as shown in Fig. 1, cells only mutate in one direction and it is not possible to have such scenario. Furthermore, we will not study the case when $x_0 = x_1 = x_2 = 0$ because we always consider $x_0 + x_1 + x_2 = 1$.

Let us seek for these three possible fixed points. Then we have to find the solutions of the following system:

$$\begin{pmatrix} 0 \\ 0 \\ 0 \end{pmatrix} = \begin{pmatrix} f_0 Q & 0 & 0 \\ f_0(1-Q) & f_1 Q' & 0 \\ 0 & f_1(1-Q') & f_2 \end{pmatrix} \begin{pmatrix} x_0 \\ x_1 \\ x_2 \end{pmatrix} - \Phi(\mathbf{x}) \begin{pmatrix} x_0 \\ x_1 \\ x_2 \end{pmatrix} \tag{4}$$

- If we consider $x_0 = x_1 = 0$ and $x_2 \neq 0$, from the system (4) we obtain $f_2 x_2 - \Phi(x_0, x_1, x_2) x_2 = 0$, which has two possible solutions $x_2 = 0$ or $x_2 = 1$. As we require the sum of the three variables to be 1, then the solution is $(x_0^*, x_1^*, x_2^*) = (0, 0, 1)$.

- Let us consider now $x_0 = 0$ and then solve the obtained system of equations:

$$\begin{cases} f_1 Q' - f_1 x_1 - f_2 x_2 = 0 \\ f_1(1-Q')x_1 + f_2 x_2 - f_1 x_1 x_2 - f_2 x_2^2 = 0 \end{cases} \tag{5}$$

  Its solution is $x_1^* = \frac{f_1 Q' - f_2}{f_1 - f_2}$ and $x_2^* = \frac{f_1 - f_1 Q'}{f_1 - f_2}$. Notice that, as x_1 and x_2 are ratios of population, x_1^* and x_2^* must take values from 0 to 1. Then, from their expressions and remembering that $0 < Q' < 1$, we get the conditions: $f_1 > f_2$ and $f_1 Q' > f_2$.

- Finally, for the last fixed point we consider $x_0 \neq 0, x_1 \neq 0, x_2 \neq 0$. Then, from the first equation of the system we have $\Phi(x_0, x_1, x_2) = f_0 Q$. Hence the new system has this form:

$$\begin{cases} f_0(1-Q)x_0 + (f_1Q' - f_0Q)x_1 = 0 \\ f_1(1-Q')x_1 + (f_2 - f_0Q)x_2 = 0 \end{cases} \tag{6}$$

  under the constraint $x_0 + x_1 + x_2 = 1$.

  Then its solution is as follows:

$$x_0^* = \frac{(f_0Q - f_1Q')(f_0Q - f_2)}{\varphi(f_0, f_1, f_2, Q, Q')}$$

$$x_1^* = \frac{f_0(1-Q)(f_0Q - f_2)}{\varphi(f_0, f_1, f_2, Q, Q')}$$

$$x_2^* = \frac{f_1(1-Q')f_0(1-Q)}{\varphi(f_0, f_1, f_2, Q, Q')}.$$

  where

$$\varphi(f_0, f_1, f_2, Q, Q') = (f_0Q - f_1Q')(f_0Q - f_2) + f_0(1-Q)(f_0Q - f_2) + (f_1(1-Q')f_0(1-Q).$$

Remark 4.1. *We can consider $f_1 = f_2$ as particular case. If these two fitness parameters are equal, the system (3) only has two possible fixed points.*

From now on, we give some results based in the solution of the system (3). To compute these solutions we have used the *Taylor* software. *Taylor* is an ODE solver generator which reads a system of ODEs and it outputs an ANSI C routine that performs a single step of the numerical integration of these ODEs, by means of the Taylor method. Each step of integration chooses the step and the order in an adaptive way trying to keep the local error below a given threshold, and to minimize the global computational effort [26].

Numerically, we integrate the solution of system (3) with initial condition $(0, 0, 1)$. The next Lemma ensures that any point of this orbit satisfies $x_0 + x_1 + x_2 = 1$. Moreover, it can be used as an accuracy control while integrating the ODE system.

Lemma 4.2. *$S = x_0 + x_1 + x_2$ is a first integral of system (3), that is* $\dfrac{dS}{dt} = 0$.

Proof. From the equations (3), we know that

$$\begin{aligned}\frac{dS}{dt} &= \dot{x_0} + \dot{x_1} + \dot{x_2} \\ &= f_0 Q x_0 + f_0(1-Q)x_0 + f_1 Q' x_1 + f_1(1-Q')x_1 + f_2 x_2 - \Phi(x_0 + x_1 + x_2) \\ &= \Phi(x_0, x_1, x_2)(1 - (x_0 + x_1 + x_2))\end{aligned}$$

Since the initial condition is $x_0 = 1$ and $x_1 = x_2 = 0$, $1 - (x_0 + x_1 + x_2) = 0$. □

As a particular case we consider $Q = 0.7$, $Q' = 0.3$ and $f_2 = 0.42$. Then we make f_0 to take values from 0.01 to $\frac{1}{Q}$ and f_1 to take values from 0.01 to $\frac{1}{Q'}$ both with a step of 0.01. We can not start with $f_0 = 0$ or $f_1 = 0$ because this way x_0 or x_1 would become extinct. So, we compute the analytical result for all the possible fixed points and, with the iterative method, we integrate the ODE until the distance between the result of the iterate and one of the fixed points is less than an error tolerance previously set, in our case ϵ^{-16}. We also fix an upper limit for the time taken by the system to reach a fixed point, therefore we consider it does not reach any fixed point if this upper limit is surpassed.

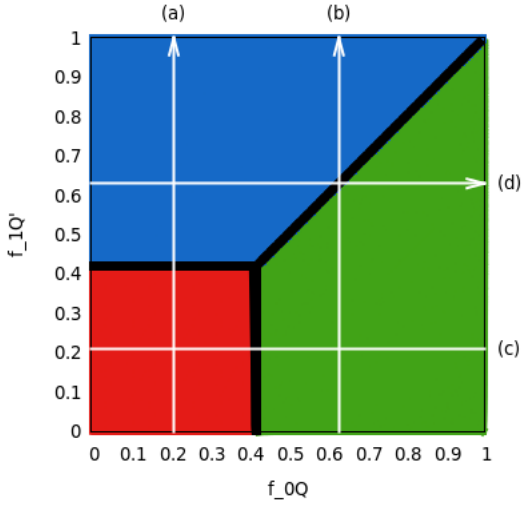

Figure 2: Analysis of the parameters space to find the fixed points. Each coloured region indicates a different fixed point (red: $(0, 0, 1)$; blue: $(0, x_1^*, x_2^*)$; and green:(x_0^*, x_1^*, x_2^*)). The thick black lines indicate that the system does not reach any fixed point. The white arrows are different sections that will be further studied.

Figure 2 shows the fixed points that are reached by the system depending on the parameters f_0Q and f_1Q'. Here each fixed point is indicated with a different colour. Red indicates that the fixed point is $x^* = (0, 0, 1)$; blue indicates that the fixed point is $x^* = (0, \frac{f_1Q'-f_2}{f_1-f_2}, \frac{f_1-f_1Q'}{f_1-f_2})$; and green indicates the fixed point where all of subpopulaions coexist. In addition, black lines indicate that none of the fixed points were reached by the system. Notice that in our analysis we are tuning f_0Q and f_1Q'. The decrease of these pair of parameters is qualitatively equivalent to the increase of mutation rates μ_0 and μ_1, respectively. For instance, going from $f_1Q' = 1$ to $f_1Q' = 0$ can be achieved increasing μ_1.

Figure 3 shows the density of each population at the equilibrium point in the same parameter space of Fig. 2. This analysis allows us to characterize the regions of this parameter space where stable cells x_0 density is high and the malignant population x_2 remains low. As Solé and Deisboeck [12] identified, this scenario can be achieved by increasing μ_1. Furthermore, our results suggest that this behaviour is robust to changes in μ_0. Notice that this behaviour is found for a wide range of f_0Q values. Furthermore, a decrease of f_0Q (or increase of μ_0) makes the population densities of x_0^* and x_2^* to decrease and increase respectively, while for this range the values of x_1^* remains low.

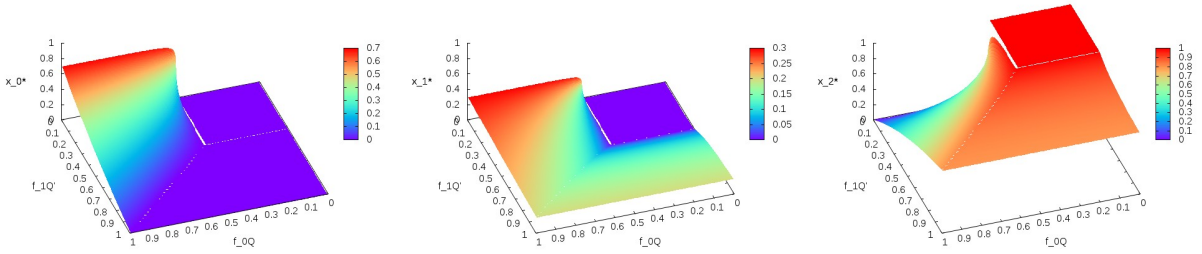

(a) (b) (c)

Figure 3: Equilibrium concentration of each variable in the parameter space (f_0Q,f_1Q'). The equilibrium value for x_0 is displayed in (a) while the population equilibria of x_1 and x_2 are shown, respectively, in (b) and (c). Notice that the color bar for each panel is not normalized.

We observe that there is a frontier between the different fixed points reached by the

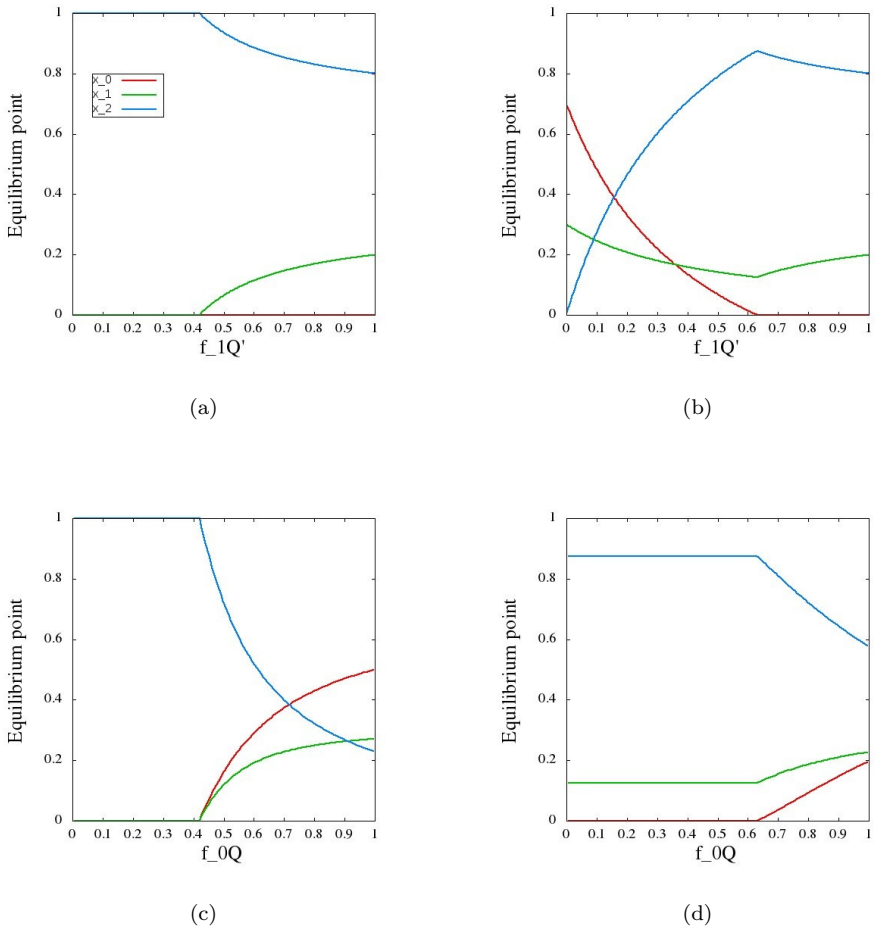

Figure 4: Impact of changing the replication fidelity of the populations x_0 and x_1, i.e., f_0Q and f_1Q' respectively. In (a) and (b) f_0Q has fixed values 0.21 and 0.63 respectively; in (c) and (d), f_1 has fixed values 0.21 and 0.63. Notice that the letter of each panel correspond to sections made in Fig. 2, represented by the white arrows.

system. The pass from one fixed point to another can be given by a bifurcation. In Fig. 4 we appreciate these bifurcations more clearly (in the next section we will study the bifurcation in detail). For this purpose, we have set four sections of Fig. 2 (white arrows), i.e., we have fixed different values for f_0 and f_1. In this case these values are $f_0Q = 0.21, 0.63$ and $f_1Q' = 0.21, 0.63$.

We see the bifurcations of the fixed points of the system in Fig. 4. In (a) and (b) f_0Q has fixed values 0.21 and 0.63 respectively, so bifurcations are represented depending on the replication fidelity of x_1 in both cases. We notice that for high replication fidelity only x_1 and x_2 coexist. But in (b) the case is different: if we study this graphic in terms of

the mutation rate of x_1 we can observe that for high values of it, the system stays at an equilibrium point where x_0 is greater. That means that if we make the mutation rate μ_1 higher through therapy it is possible to make the tumor to achieve an equilibrium state where the most unstable cells are near to 0 and the whole population is mainly dominated by x_0.

In cases (c) and (d) we have considered fixed values $f_1Q' = 0.21$ and $f_1Q' = 0.63$ and, therefore, now bifurcations are represented in terms of the replication fidelity of x_0. Notice that in both cases the higher is the probability of x_0 to stay stable (equivalently, the mutation rate μ_0 of x_0 is low) the higher is the population of stable cells at the equilibrium point. This is crucial since they correspond to final scenarios with an important presence of genetically stable cells. Comparing these cases, we observe that, if the mutation rate of x_1 is higher, i.e., case (c) ($f_1Q' = 0.21$, i.e., $f_1\mu_1 = 0.49$), the population x_0 in the equilibrium point reached is also higher. This suggests the existence of a threshold in the unstability of x_1 bringing more stable cells x_0 in the final equilibria.

4.2 Stability analysis and bifurcations

The stability of the points found in the previous section 4.1 is performed by using the Jacobi matrix:

$$L_\mu(x^*) = \begin{pmatrix} f_0Q - \Phi(\mathbf{x}) - x_0f_0 & -x_0f_1 & -x_0f_2 \\ f_0(1-Q) - x_1f_0 & f_1Q' - \Phi(\mathbf{x}) - x_1f_1 & -x_1f_2 \\ -x_2f_0 & f_1(1-Q') - x_2f_1 & f_2 - \Phi(\mathbf{x}) - x_2f_2 \end{pmatrix} \tag{7}$$

We are specially concerned with the domain, in the parameter space, where the malignant cells become dominant and the stability of such equilibrium state. Thus, taking $x^* = (0, 0, 1)$, the Jacobi matrix has the following eigenvalues:

$$\lambda_1 = f_0Q - f_2, \lambda_2 = f_1Q' - f_2, \lambda_3 = -f_2 \tag{8}$$

So, x^* is an attractor if the two inequalities, $f_0Q < f_2$ and $f_1Q' < f_2$, are satisfied.

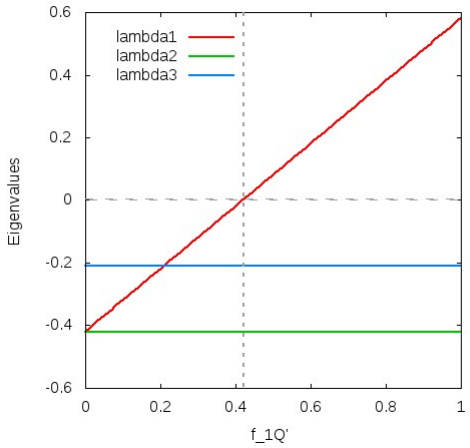

Figure 5: Eigenvalues of $L_\mu(x^*)$ for $x^* = (0, 0, 1)$ and $f_0Q = 0.21$, using the range of the arrow (a) in Fig. 2.

From the expression of the eigenvalues we conclude that there is a critical condition for the mutation rates $\mu_0 = 1 - Q$ and $\mu_1 = 1 - Q'$: $\mu_0^c = 1 - \frac{f_2}{f_0}$ and $\mu_1^c = \frac{f_2}{f_1}$. These conditions separate the domain where only x_2 remains from the other two cases. From Fig. 5 we confirm that the fixed point $x^* = (0, 0, 1)$ is an attractor point until this critical condition i.e., the error threshold, (shown by a vertical dotted line) is reached.

If we study the fixed point $x^* = (0, \frac{f_1Q'-f_2}{f_1-f_2}, \frac{f_1-f_1Q'}{f_1-f_2})$ we get the following eigenvalues from the Jacobi matrix:

$$\lambda_1 = f_0Q - f_1Q', \lambda_2 = \frac{f_1(f_2 - f_1Q')}{f_1 - f_2}, \lambda_3 = \frac{2f_1f_2Q' - f_1^2Q' - f_2^2}{f_1 - f_2} \tag{9}$$

Notice that, as we mention in Remark 4.1, when $f_1 = f_2$, such fixed point does not exist, hence the eigenvalues of the Jacobi matrix do not exist neither. This can be appreciated from Fig. 6, when $f_1Q' = 0.126$, thus $f_1 = f_2 = 0.42$. We also have a critical condition for this case and it can be appreciated in Fig. 6 with the dotted vertical line.

Finally, we want to study the stability of the fixed point where all populations coexist. An analytical expression for the eigenvalues exists, since we have the Jacobi matrix and the analytical expression for the fixed point itself. But they have really complicated

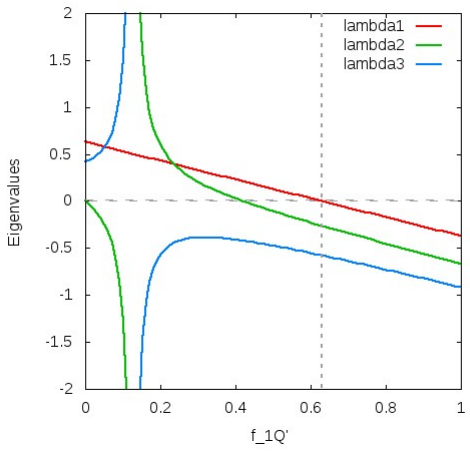

Figure 6: Eigenvalues of $L_\mu(x^*)$ for $x^* = (0, x_1^*, x_2^*)$ and $f_0 Q = 0.63$.

expressions and, even more, we are considering $n = 1$. This means that the greater n, the analytical expressions for the eigenvalues are more complicated to find. This is the reason why it is interesting to compute them numerically.

To compute the eigenvalues of this 3-dimensional matrix we proceed in the following way. This procedure turns to be quite fast in our case (dimension 3) but is not applicable for higher dimensions. It works as follows:

- We first apply the *power method* to compute an approximation for the eigenvalue of maximal modulus. As it is known, it is based on the idea that the sequence $v_{k+1} = Av_k$ should behave for large values of k as the direction of the eigenvector associated to the largest (in modulus) eigenvalue $\lambda_{\max}$ of A. To compute it one starts from an arbitrary initial vector v_0 (in our case, for instance, $(1/3, 1/3, 1/3)$ and computes $v_{k+1} = Av_k$. Provided the difference between the largest eigenvalue and the second largest eigenvalue (in modulus, always) is not too small, the quotients of the components of v_{k+1}, v_k, that is $v_{k+1}^{(j+1)}/v_{k+1}^{(j)}$, converge to $\lambda_{\max}$. To avoid problems of overflow one normalizes v_{k+1}, i.e. $w_{k+1} = v_{k+1}/ \parallel v_{k+1} \parallel$, at any step. Problems of convergence appear when the two largest eigenvalues of A are close.

- We apply the same method to A^{-1} to obtain the smallest eigenvalue of A, since λ is eigenvalue of A iff λ^{-1} is eigenvalue of A^{-1}. To compute A^{-1} we have used its

QR-decomposition, which writes A as the product of two matrices: an orthogonal matrix Q and an upper triangular matrix R, i.e., $A = QR$.

- Provided $\lambda_{\max}$, $\lambda_{\min}$ are accurate enough, the third eigenvalue is determined from the value of the determinant of the matrix A, that we have derived from its QR-decomposition.

We apply this procedure to the study of possible bifurcations in the stability of the equilibrium points obtained when we do not have analytic expressions for the associated eigenvalues. To show it we fix a value for f_0Q and move f_1Q'. We have chosen a value for f_0Q corresponding to the line (b) of the diagram in Fig 2. Observe that, when moving at the green zone our equilibrium point is of the form $(x_0^*, x_1^*, 1 - x_0^* - x_1^*)$ while it is of the form $(0, x_1^*, 1 - x_1^*)$ when we move along the blue one. For each equilibrium point, whose components depend on f_1Q', we compute its differential matrix and its associated eigenvalues. These eigenvalues, computed numerically as mentioned above, are plotted in Fig. 7. They are all three real. Observe that there is an interchange of the number of positive and negative eigenvalues around the bifurcation value 0.63, but no change in their stability. They are always unstable since we have at least one eigenvalue positive.

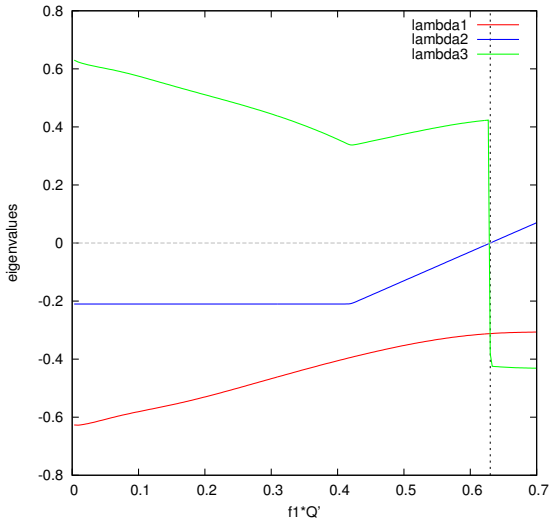

Figure 7: Eigenvalues of the differential at the equilibrium point as a function of f_1Q'. The vertical dotted line corresponds to the bifurcation value 0.63.

It is interesting to highlight the change in the geometry of such equilibrium point: for values of f_1Q' under the bifurcation value 0.63 its invariant stable manifold is 2-dimensional and its invariant unstable manifold 1-dimensional; on the contrary, after the bifurcation the associated dimensions of the invariant manifolds are exchanged. In both cases, the orbit starting at initial conditions $(1, 0, 0)$ finishes at the stable manifold of that equilibrium point.

4.3 Transient times

In this section we study the time taken by the system to reach one of the fixed points found in section 4.1. Typically, the behaviour of transient times change near bifurcation thresholds, and, particularly for our system, we are interested in possible changes in transients due to changes in mutation rates. These phenomena could be relevant in patient response under mutagenic therapy.

Figure 8 shows the same as Fig. 2, in the sense that we iterate the same parameters of the system, but it represents the transient times. Here we use the same method to integrate the ODE system, but taking into account only the time taken to reach an equilibrium point. Notice that if we observe the contour lines represented at the bottom of Fig. 8 we have the same as in Fig. 2. This means that the "time to equilibrium" of the system increases when we are near bifurcation points, which are represented with black lines in Fig. 2.

When slightly modifying the mutation rate of x_1 near the error threshold, we see that the time taken by the tumor to reach an equilibrium state is significantly lower. In particular, when increasing the mutation rate, not only time decreases but also we see that the tumor reaches an equilibrium point where the stable cells population is higher. This can be appreciated in Fig. 9, where red, green and blue lines represent x_0, x_1 and x_2 respectively and the dashed, orange line represents the time, which is rescaled to be able to relate it with the corresponding equilibrium point. In case of possible mutagenic therapies directly targeting the most unstable cells, our results reveal that no large increments of

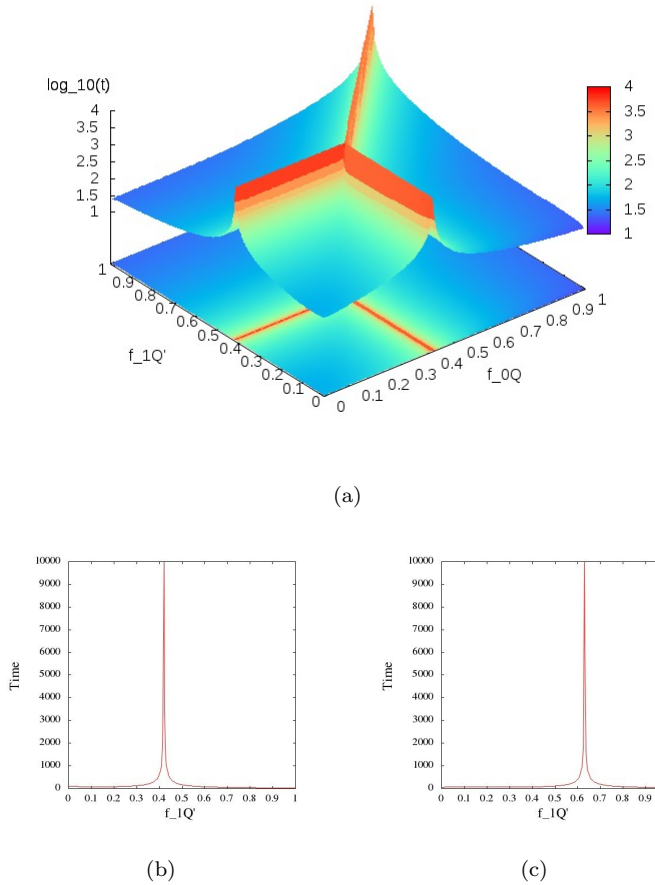

(a)

(b) (c)

Figure 8: Time taken by the system to reach a fix point in the parameter space (f_0Q,f_1Q'). Time in (a) is logarithmic represented in base 10 but in sections (b) and (c) it is represented in real scale due to appreciate the actual velocity of the system.

mutation may be needed to achieve the error threshold and thus the desired state, i.e., x_0 population dominates.

When rescaling Fig. 8 (b) in terms of logarithm in base 10 (as we can see in Fig. 9) if we increase the mutation rate of x_1, time decreases faster than an exponential function, which is interesting result since it implies an equilibrium scenario with a dominant presence of x_0 that can be reached with a short time.

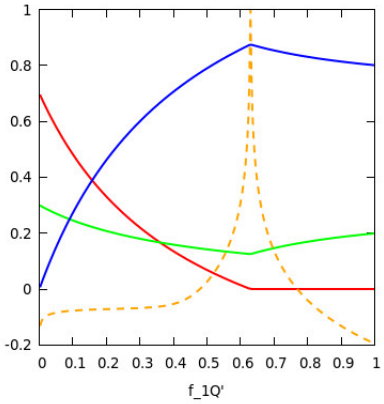

Figure 9: The dashed line corresponds to $\frac{log_{10}(t)-2}{2}$, and the solid lines are the equilibrium densities of x_0 (red), x_1 (green) and x_2 (blue) for $f_0Q = 0.63$. Notice that the time maximum at the bifurcation value.

5 Conclusions

In this Bachelor's degree thesis we study an ODE system modelling the behaviour of a population of tumor cells with a mean-field quasispecies model introduced by Solé and Deisboeck [12]. Thus, in our simplified model we have assumed the following: the model does not consider stochasticity and does not take into account spatial correlations between cells as well. Even more, we do not consider cell death, otherwise we model competition in terms of replication and mutation.

First, we have found the fixed points of the system analytically and we have studied their stability both analytically and numerically. We have also characterized the bifurcations between the different fixed points. We conclude that, depending on the parameters, the system can reach equilibrium states where tumoral cells decrease their population density while stable cells population dominates. This scenario can be achieved increasing the level of genetic instability conferred through the mutation rate μ_1 of the mutator-phenotype population x_1. If this mutation rate exceeds the so-called error threshold, the replication rate of the more malignant subpopulation x_2 is reduced to a point where it has no longer competitive advantage.

Further analysis of the effects of mutation rate μ_1 on the dynamics of the system have allowed us to determine a transcritical bifurcation. Under such a bifurcation, the time

taken by the system to reach the desired equilibrium state is shown to drastically decrease with slight changes in the mutation rate μ_1 near the error threshold. This result can give us a clue about how medication and therapy may affect the tumor behaviour in case of direct mutagenic therapies against tumor cells. In other words, it is possible to modify the mutation rate of the cells through therapy, and we have seen that if we slightly increase the mutation rate of x_1 near the error threshold we can obtain an equilibrium point with a dominant population of stable cells rapidly.

The code used to obtain the results among this work is available upon request.

References

[1] Cairns, J., 1975, Mutation selection and the natural history of cancer. Nature 255, 197-200.

[2] Merlo, L.M.F., Pepper, J.W., Reid, B.J., Maley, C.C., 2006. Cancer as an evolutionary and ecological process. Nature Rev. Cancer 6, 924-935.

[3] Cahill, D.P., Kinzler, K.W., Vogelstein, B., Lengauer, C., 1999. Genetic instability and darwinian selection in tumors. Trends Genet. 15, M57–M61.

[4] Loeb, L.A., 2001. A Mutator Phenotype in Cancer. Cancer Res. 61, 3230–3239. http://cancerres.aacrjournals.org/content/61/8/3230.long

[5] Oliver, A., Canton, R., Campo, P., Baquero, F., et al., 2000. High frequency of hypermutable Pseudomonas aeruginosa in cystic fibrosis lung infection. Science 288, 12514.

[6] Bjedov, I., Tenaillon, O., Gérard, B., Souza, V., et al., 2003. Stress- induced mutagenesis in bacteria. Science 300, 14049. 35.

[7] Sniegowski, P.D., Gerrish, P.J., Lenski, R.E., 1997. Evolution of high mutation rates in experimental populations of E. coli. Nature 387, 7035.

[8] Anderson, G.R., Stoler, D.L., Brenner, B.M., 2001. Cancer as an evolutionary consequence of a destabilized genome. Bioessays 23, 103746.

[9] Bielas, J.H., Loeb, K.R., Rubin, B.P., True, L.D., et al., 2006. Human cancers express a mutator phenotype. Proc. Natl. Acad. Sci. USA 103, 18238-18242.

[10] Hoeijmakers, J.H., 2001. Genome maintenance mechanisms for preventing cancer. Nature 411, 366-374.

[11] Benedikt, B., Siebert, R., Traulsen, A., 2014. Cancer initiation with epistatic interaction between driver and passenger mutations. J. Theor. Biol. 358, 52-60.

[12] Solé R.V., 2001. Phase transitions in unstable cancer cells populations. The European Physics Journal B. 35, 117–123.

[13] Brumer, Y., Michor, F., Shakhnovich, E.I., 2006. Genetic instability and the quasispecies model. J. Theor. Biol. 241, 216–222. http://michorlab.dfci.harvard.edu/publications/JTheorBiol2006_6.pdf

[14] Eigen, M., 1971. Selforganization of matter and evolution of biological macromolecules. Naturwissenschaften 58, 465-523.

[15] Eigen, M., Schuster, P., 1979. The hypercycle: a principle of natural selforganization (Springer-Verlag New York). Naturwissenschaften 58, 465-523.

[16] Solé, R.V., Sardanyés, J., Díez, J., Mas, A., 2006. Information catastrophe in RNA viruses through replication thresholds. J. Theor. Biol., 240, 353-359.

[17] Cichutek, K., Merget, H., Norlay, S., Linde, R., et al., 1992. Development of a quasispecies of human immunodeficiency virus type 1 *in vivo*. Proc. Natl. Acad. Sci. USA, 89, 7365-7369.

[18] Domingo, E., Biebricher, C.K., Eigen, M., Holland, J.J., 2001. Quasispecies and RNA virus evolution: principles ans consequences. Landes Bioscience, Georgetown Texas.

[19] Bull J.J., Sanjuán R., Wilke C.O., 2007. Theory of lethal mutagenesis for viruses. J. Virol. 81, 2930–2939. http://jvi.asm.org/content/81/6/2930.long

[20] Wylie, C.S., Shakhnovich, E.I., 2012. Mutation Induced Extinction in Finite Populations: Lethal Mutagenesis and Lethal Isolation. PLoS Comput. Biol 8(8), e1002609. http://www.ploscompbiol.org/article/info%3Adoi%2F10.1371%2Fjournal.pcbi.1002609

[21] Lauring, A.S., Andino, R., 2010. Quasispecies Theory and the Behavior of RNA Viruses. PLoS Pathog. 6(7), e1001005. http://www.plospathogens.org/article/info%3Adoi%2F10.1371%2Fjournal.ppat.1001005

[22] Sardanyés, J., Simó, C., Martínez, R., Solé, R. V. and Elena, S.F., 2014. Variability in mutational fitness effects prevents full lethal transitions in large quasispecies populations. Nature Scientific Reports 4, 4625 http://www.nature.com/srep/2014/140409/srep04625/full/srep04625.html

[23] Crotty, S., Cameron, C.E., Andino, R., 2001. RNA virus error catastrophe: Direct molecular test by using ribavirin. Proc. Natl. Acad. Sci. USA, 98, 6895-6900.

[24] Solé R.V., Deisboeck T.S., 2004. An error catastrophe in cancer?. J. Theor. Biol. 228, 47–54. http://complex.upf.es/~ricard/ERRORCATASTROPHE_JTB.pdf

[25] Swetina, J., Schuster, P., 1982. Self-replication with errors. A model for polynucleotide replication. Biophys. Chem. 16, 329–345.

[26] Jorba, Á., Zou, M., 2004. A software package for the numerical integration of ODEs by means of high-order Taylor methods. http://www.maia.ub.es/~angel/taylor/taylor.pdf

[27] Nowak, M.A., 1992. What is a quasispecies?. Trends in Ecology and Evolution 7, 118-121. http://www.ped.fas.harvard.edu/people/faculty/publications_nowak/TEE92.pdf

[28] Usher, M.B., 1971. *Developments in the Leslie model in mathematical models in ecology*. Blackwell Scientific Publications.

[29] Lux, T., Morales-Arias, L., Sattarhoff, C., 2011. A Markov-switching Multifractal Approach to Forecasting volatility. Kiel Working Paper, 1737.

[30] Forney, G.D., 1973. The Viterbi algorithm. Proceedings of the IEEE, 61, 268-278.

[31] Sergey, B., Lawrence, P., 1998. The anatomy of a large-scale hypertextual Web search engine. Computer Networks and ISDN Systems, 33, 107-117. http://infolab.stanford.edu/pub/papers/google.pdf

[32] Bryan, K., Leise, T., 2006. The $25,000,000,000$ eigenvector. The linear algebra behind Google. SIAM Review, 48 (3), 569-81. `http://www.rose-hulman.edu/~bryan/google.html`

[33] Wodarz, D., Komanova, N.L., 2005. *Computational Biology of Cancer: Lecture Notes and Mathematical Modeling.*